HHS Public Access

Author manuscript

Acta Biomater. Author manuscript; available in PMC 2016 July 19.

Published in final edited form as:

Acta Biomater. 2011 August ; 7(8): 3094–3100. doi:10.1016/j.actbio.2011.04.010.

Synthesis of a Novel Photopolymerized Nanocomposite Hydrogel for Treatment of Acute Mechanical Damage to Cartilage

Kathryn Schlichting[a], **Trishelle M. Copeland-Johnson**[b], **Matthew Goodman**[a], **Robert J. Lipert**[c], **Tanya Prozorov**[f], **Xunpei Liu**[e], **Todd O. McKinley**[d], **Zhiqun Lin**[a], **James A. Martin**[d], and **Surya K. Mallapragada**[a,e,f,*]

[a]Department of Materials Science and Engineering, Iowa State University

[b]Department of Chemical Engineering, University of South Florida

[c]Institute for Combinatorial Discovery, Iowa State University

[d]Department of Orthopaedic Surgery and Rehabilitation University of Iowa

[e]Department of Chemical and Biological Engineering, Iowa State University

[f]Division of Materials Sciences and Engineering, Ames Laboratory

Abstract

Intraarticular fractures initiate a cascade of pathobiologic and pathomechanical events that culminate in posttraumatic osteoarthritis (PTOA). Hallmark features of PTOA include destruction of the cartilage matrix in combination with loss of chondrocytes and acute mechanical damage (AMD). Currently, treatment of intraarticular fractures essentially is completely focused on restoration of the macroanatomy of the joint. However, current treatment ignores AMD sustained by cartilage at the time of injury. We are exploring aggressive biomaterial-based interventions designed to treat the primary pathologic components of AMD. This study describes the development of a novel injectable copolymer solution that forms gels at physiological temperatures that can be photocrosslinked, and can form nanocomposite gels insitu through mineralization. The injectable copolymer solution will allow the material to fill cracks in the cartilage after trauma. The mechanical properties of the nanocomposite are similar to that of native cartilage, as measured by compressive and shear testing. It thereby has the potential to mechanically stabilize and restore local structural integrity to acutely injured cartilage. Additionally, the insitu mineralization ensures good adhesion at the interface between the biomaterial and cartilage, as measured through tensile and shear testing. Therefore, we have successfully developed a new injectable insitu forming nanocomposite with mechanical properties of similar magnitude to that of native cartilage, and which can bond well to native cartilage. This material has the potential to stabilize injured cartilage and prevent PTOA.

*Corresponding Author Contact: Surya Mallapragada, Stanley Professor and Chair, Department of Chemical and Biological Engineering, 2114 Sweeney Hall, Iowa State University, Ames, IA 50011-2230, 515-294-7407, Fax: 515-294-2689, suryakm@iastate.edu.

Keywords

nanocomposite; hydrogel; biomaterials; injectable

1. Introduction

Intraarticular fractures initiate a cascade of pathobiologic and pathomechanical events that culminate in posttraumatic osteoarthritis (PTOA) [1–5]. Hallmark features of PTOA include destruction of the cartilage matrix in combination with loss of chondrocytes [6–12]. The etiology of PTOA is multifactorial, but a major pathoetiologic component hypothesized to incite and propagate this destructive cascade is acute mechanical damage (AMD) sustained by the cartilage at the time of injury [12–15]. AMD affects the structural integrity of the cartilage, causes chondrocyte metabolic dysfunction, and causes chondrocyte death [7, 14, 16–18]. Chondrocytes subjected to pathological strains become increasingly metabolically incompetent or die, and no longer produce effective matrix molecules. This, in turn, leads to further matrix damage and further chondrocyte death. This damaged relationship becomes self-propagating, and has been hypothesized to cause PTOA.

Currently, treatment of intraarticular fractures is completely focused on restoration of the macroanatomy of the joint [3, 23, 24]. The treatment premise is that restoring the macroanatomy of the joint will prevent ongoing pathomechanical stresses and this will in turn prevent cartilage degeneration. Articular fragments are reduced, and metaphyseal disruptions are realigned to restore the congruity, stability, and alignment of the injured joint. However, current treatment ignores AMD sustained by cartilage at the time of injury. Furthermore, the outcomes of intraarticular fractures treated with even the most sophisticated techniques have not improved appreciably in decades (Figure 1). Taken together, the next significant improvement in outcomes of intraarticular fractures will likely involve developing effective treatment measures aimed to mitigate AMD.

We propose that a new paradigm in treating intraarticular fractures is necessary to improve outcomes. We have hypothesized that restoration of native mechanical properties to impact-injured cartilage can reduce chondrocyte death and improve chondrocyte metabolic dysfunction after an impact injury. The premise is that in the acute and subacute period after an intraarticular fracture, there is a continuum of injury among the chondrocytes in the region of AMD. Within this continuum of injury, there is a population of chondrocytes that are injured, but have potential to heal and become metabolically productive if they receive appropriate treatment. We propose that impact-injured chondrocytes have the potential to heal if they are protected from ongoing AMD-related hazardous strains. Furthermore, injured chondrocytes could also be nurtured by local delivery of therapeutic chondrocyte-enhancing bioactive agents. Maximizing the number of metabolically competent chondrocytes in regions of AMD has potential to mitigate or arrest the self-propagating cascade leading to PTOA.

We conceived that a material that could penetrate the interstitium of damaged cartilage, bond with surrounding cartilage, and restore local material properties could shield injured chondrocytes from ongoing injury-related hazardous strains which could determine whether

an injured chondrocyte proceeds to cell death, or recovers and becomes biologically productive. Furthermore, such a material could also deliver chondrocyte-enhancing bioactive agents to locally injured chondrocytes. The strategy is simple: deliver mechanical and biologic treatment preferentially into regions of AMD (matrix cracks and fracture edges). However, it requires the development of a biomaterial that can fill the cracks in the cartilage, exhibit mechanical properties similar to that of native cartilage, and good binding with the cartilage. This study describes the development of such an injectable nanocomposite photopolymerizing copolymer that has potential to restore local structural integrity to acutely injured cartilage, and subsequently act as a carrier for chondrocyte-enhancing bioactive agents. This material-design is based on our earlier work on the development of novel injectable nanocomposites formed by self-assembling polymers with attached mineralization peptides acting as templates for the nucleation and growth of inorganic nanocrystals [25–27]. In this investigation, we have designed this material to be formulated as a liquid, photopolymerized into a solid, and can develop material properties that are of the same magnitude as native cartilage. In this study, we describe the synthesis of the material and optimization of material properties to meet our requirements listed above.

2. Materials and Methods

2.1 Materials

Specific materials used in this project include PEG-1000 [Poly (ethylene glycol) 1000 dimethacrylate] (Fp: 220°F, Specific Gravity: 1.1) synthesized by Polysciences, Inc. (Warrington, PA). The Pluronic F-127 Copolymer [poly (ethylene oxide) –*b*– poly (propylene oxide) –*b*– poly (ethylene oxide)] (MW_n: 12,600 Da) was a product of BASF Corp. (Florham Park, NJ). *N*-hydroxysuccinimide (NHS) [MW: 115.09 g/mol, ≥97% Purity and succinic anhydride MW: 100.1, were obtained from Sigma-Aldrich (St. Louis, MO)]. The Collagen Binding Peptide (CBP) (GLRSKSKKFRRPDIQYPDATDED…) (97.9% Purity, MW: 3292.71) and calcium phosphate binding peptide (HAp) (DSKSDSSKSESDSS) (~95% Purity, MW: 1445 Da) were synthesized by Genscript Corporation (Piscataway, NJ). Pyridine [MW: 79.1 certified ACS grade], anhydrous diethyl ether [MW: 74.1], toluene [MW: 92.1 certified ACS grade], and dichloromethane [MW: 84.9 pesticide grade] were purchased from Fisher Scientific (Hanover Park, IL). *N*,*N*′-dicyclohexylcarbodiimide [MW: 206.3] was from Avocado Research Chemicals (Lancashire, UK). The photoinitiator for assistance in cross-linking hydrogel formation was Igracure® 2959 [4-(2-hydroxyethoxy) phenyl – (2-hydroxy-2-propyl) ketone] (MW: 224 g/mol) synthesized by Ciba AG-CH (Basel, Switzerland). Cartilage samples were obtained from bovine patellae obtained from a local slaughterhouse. The patellae were kept frozen and then thawed at room temperature prior to sample preparation. The Omnicure Series 1000 IB UV radiation lamp used for photo cross-linking was manufactured by EXFO Photonic Solutions, Inc. (Quebec City, Canada).

2.2 Nanocomposite Synthesis

The hydroxyl end groups of Pluronic were converted to carboxyl groups by treating with succinic anhydride in pyridine as reported in the literature [28]. Pluronic (32 g, 2.5 mmol) and succinic anhydride (1 g, 10 mmol) were dissolved in pyridine (100 mL), and the reaction was carried out at 40 °C for 24 hours. The mixture was then precipitated in diethyl

ether, dissolved in toluene, and reprecipitated in diethyl ether. The product was then dried under vacuum. The carboxyl-terminated Pluronic was esterified with NHS as reported in literature [29]. To a round-bottom flask connected with an argon line and bubbler, Pluronic (0.128 mmol), 0.0792 g of *N,N*-dicyclohexylcarbodiimide (3 x excess, 0.384 mol), 0.0442 g of NHS (3 x excess, 0.384 mol), and 8 mL of dichloromethane were added. The reaction was carried out at room temperature for 24 h. The reaction mixture was then filtered and precipitated in cold diethyl ether. The NHS attachment was verified by 1H NMR with ester peak at approximately 2.7 ppm and was found to be around 1% (wt/vol). The NHS-functionalized polymer was then conjugated with the HAp peptide and/or the CBP peptide. NHS polymer (1.5 g) was added to a solution of 12 mg of peptide in 50 mL of PBS (pH 7.4) with stirring at room temperature. After 4 hours, an additional 1.5 g of NHS-polymer was added to the mixture. The reaction was maintained at room temperature for 24 hours. The reaction mixture was dialyzed against water using a cellulose ester membrane with a molecular weight cutoff of 3500 (Spectrum Labs, Rancho Dominguez, CA) for 48 hours to remove the uncoupled peptide. The polymer-peptide solution was then lyophilized, a pure white powder was obtained, and the peptide attachment was then qualitatively characterized with 1H NMR.

The nanocomposite gels were synthesized by following a general procedure, as shown in Figure 2. First, 90 mg of PEG-1000, followed by either 30 mg of an F-127 Pluronic attached to either CBP or HAp, or 15 mg each of Pluronic attached of CBP and HAp, were added to a labeled 20 mL scintillation vial. Afterwards, 250 μL of a 4M Ca^{+2} ($CaCl_2.2H_2O$) solution, mixed with 104 mg of the Igracure photoinitiator, was added. The vials were then refrigerated for 24 hours. After that time, the contents of each vial were stirred on a vortex machine to achieve a homogenous composition, and 150 μL of a 4M PO_4^{-3} ($(NH_4)_2HPO_4$) solution was added, to promote the nucleation and growth of calcium phosphate nanocrystals. Non-mineralized gel-making solutions used for producing control samples were generated by replacing both the Ca^{2+} and PO_4^{3-} solutions with 400 μL of deionized water containing dissolved photoinitiator. All vials were returned to refrigeration for another 24 hours.

Nanocomposite samples were then produced by photocrosslinking uniform amounts of these polymer solutions above in ½″ 10 mm outer diameter glass tubes placed in a Petri dish under a UV irradiation lamp for 120 seconds at 50 mW/cm^2. A selected group of both mineralized and non-mineralized hydrogels were generated by depositing the gel-making solutions on bovine cartilage disks placed at the bottom of the glass tubes. Synthesized hydrogels were then allowed to swell in a phosphate buffered saline solution (PBS) (7.2 pH; 0.1M Na_3PO_4 and 0.15 M NaCl). Samples were then characterized and tested after aging for 24 and 48 hours.

The crystal structure of the nanocomposite was investigated by X-ray diffraction (XRD) (X'Pert PRO, PANalytical Inc., Westborough, MA,). The diffractometer was operated at 45 kV and 40 mA. CuKα radiation with a wavelength of 0.15418 nm was employed. The scan rate was 0.021°/s with a step size of 0.017° over the range of $10° \leq 2\theta \leq 80°$.

The percentage of inorganic material in the nanocomposite was determined by thermogravimetric analyzer (TGA 7, Perkin Elmer). Approximately 15 mg of the hydrogel nanocomposite sample was placed in a platinum pan, and was heated from 20 °C to 700 °C at a rate of 10 °C/min under 20 ml/min nitrogen flow condition.

Transmission Electron Microscopy analysis was performed with the Tecnai G^2 F20 Scanning Transmission Electron Microscope (STEM) (FEI Company, Hillsboro OR) equipped with High Angle Annular Dark Field (HAADF) and Energy Dispersive X-ray Spectroscopy (EDS) detectors at operating voltage 200 KV.

20 micrograms of the ground photocrosslinked solid specimen were dispersed in 5 mL of ddH_2O and left in the liquid for 24 hours to ensure the removal of the organic matrix. 2 mL of ddH_2O were then added to the 100 μl of the suspension prepared in this manner. 20 μl of a diluted specimen suspension were deposited on a carbon-supported Quantifoil copper grid. To determine the average size of the particles in the nanocomposite, multiple areas of each specimen were examined. Imaging of the nanocomposite specimens was performed without staining with the bright field (BF) TEM mode.

2.3. Mechanical testing

2.3.1 Compressive Modulus Testing—The static compressive modulus of elasticity was determined in five samples using a dynamic mechanical analyzer (DMA 7, Perkin Elmer). Five mm diameter disk samples of the materials were used that were between 1–2 mm in height. A 0–2000 mN compressive force was applied at 30 mN/min. The five separate specimens were synthesized with duration of photocrosslinking ranging between 120 seconds and 1000 seconds, and the intensity of the photocrosslinking energy ranging between 20 to 50 mW. Two bovine cartilage specimens were tested as control samples.

2.3.2 Shear Testing—Shear testing was conducted using an ARES RFS Rheometer manufactured by TA Instruments (New Castle, DE), utilizing 8 mm Stainless Steel Parallel Plate Geometry combined with a coquette bob fixture for submerging samples within PBS Buffer during testing. Samples were subjected to Dynamic Strain Sweep (DSS) testing. All tests were conducted at room temperature, at a frequency of 63 rad/s, with the strain varying from 1 to 70% at increments of 1% using a linear sweep mode. Four experimental samples were tested. The first two experimental specimens were fully mineralized samples either with or without collagen binding peptides added to the hydrogel. The second two experimental specimens were composite structures fabricated by bonding fully mineralized samples of the hydrogel to mating samples bovine patellofemoral cartilage. These composite hydrogel-cartilage samples were tested to determine how effectively the material bonded to cartilage. Shear tests of composite samples quantified how the composite material-cartilage structure resisted shearing load and where the shearing deformation occurred. Non-mineralized variations of the hydrogel samples with or without collagen binding peptides were also tested to determine the effect of mineralization. Bovine patellofemoral cartilage served as control tissue.

2.3.3 Tensile Testing—To determine how well the hydrogel enhanced with collagen binding peptides formed tensile bonds with cartilage, tensile testing was performed on the

fully mineralized hydrogel sample loaded with collagen binding peptides that was bonded to a bovine cartilage sample. For this, the fully mineralized samples containing collagen binding peptides deposited on bovine cartilage were attached to the disc sample holder of the DMA using superglue. The sample was then lowered until contact was made with the lower plate and attached. Subsequently, the cartilage and hydrogel were compressed for 5 minutes at 10mN force. The tensile force, applied at 100 mN/min, was measured to determine the adhesion strength at the interface between the cartilage and the hydrogel. Two other tests were conducted: one a mineralized sample of the hydrogel without any binding peptides attached to a piece of cartilage and one without mineralization with the HAp containing hydrogel.

2.3.4. Statistical Analysis—To determine if the different data sets were significant, a 2-tailed t-test was used with the alpha value of 0.1 and n-1 degrees of freedom with n=5 as the sample size.

3. Results

3.1 Nanocomposite Characterization

TGA results obtained by heating the material to 700°C showed a 15 wt% inorganic content in the gels. Analysis in the BF TEM mode revealed well-formed rounded nanoparticles of the inorganic phase with a mean particle size of approximately 40 nm (Fig. 3). XRD results (not shown) confirmed that the inorganic phase was brushite, a form of calcium phosphate.

3.2 Compression Testing

Compression testing of the mineralized material demonstrated compressive moduli of similar magnitude to bovine cartilage (Figure 4). The mineralized material compressive modulus ranged between 0.64 ± 0.1 MPa compared to 0.35 ± 0.1 MPa for bovine cartilage. Statistically, the difference in the average strain values was significant at or below 7 percent strain. In a series of tests (not shown), varying the photopolymerizing energy from 25 mW/cm^2 to 250 mW/cm^2 and exposure time between 30 seconds and 5 minutes had little effect on the compressive modulus on five separate specimens. All specimens were modestly stiffer than bovine cartilage. To adjust the compressive strength, the concentration of hydroxyapatite binding peptides can be altered.

3.3 Shear Testing

Shear testing was conducted on isolated samples of the mineralized material with or without addition of collagen binding peptides. Non-mineralized variations of the hydrogel samples that acted as controls provided critical information on the impact of mineralization and the contribution of CBP and HAp to the mechanical strength of the hydrogel materials. Non-mineralized samples containing only HAp were unable to withstand loading force for rheological testing, nor bonded properly when interfaced with cartilage. In contrast, non-mineralized HAp/CBP samples resisted shear loading, but did not effectively bond to bovine cartilage. All differences were found to be statistically significant using the p-value of 0.1.

Mineralization significantly increased the shear strength of the material. Mineralized samples demonstrated modestly stiffer shear moduli compared to bovine cartilage (Figure 5). However, gross deformation features of the mineralized samples and cartilage were very similar (Figure 5). The shear modulus of bovine cartilage at 20% strain was approximately 0.7 GPa compared to 1.5 to 2 GPa in the four experimental specimens. Addition of collagen binding peptides did not affect the shear moduli of the mineralized material. Subsequently, we tested a composite structure consisting of the mineralized material bonded to a piece of bovine cartilage. This test was conducted to determine how well the copolymer bonded to cartilage. These tests demonstrated excellent bonding characteristics to cartilage with shear moduli again modestly stiffer than native cartilage, but with similar deformation characteristics (Figure 5). Furthermore, shear deformation occurred uniformly through the material and cartilage, and was not preferentially concentrated at the bonding interface between the material and cartilage. G* response curves for hydrogel and cartilage samples bear more of a resemblance to that of G′ than G″.

Tan δ responses (Figure 6) for cartilage and mineralized experimental samples were directly proportional to strain magnitude. Increases in tan δ (the ratio of viscous deformation/elastic deformation in a viscoelastic material) indicate a material is becoming more viscous with increased deformation. As strain increased, the mineralized hydrogel remained more elastic than native cartilage. Furthermore, the composite samples of the mineralized material bonded to cartilage were particularly resistant to increasing viscous behavior at higher strains (Figure 6).

3.4 Tensile Testing

The tensile modulus measured 0.9 ± 0.1 MPa in bovine cartilage compared to 0.5 ± 0.1 MPa in the bovine cartilage bonded to the mineralized material loaded with HAp or 0.4 ± 0.05 MPa with carboxyl end groups (Figure 7). These measured values are statistically significant with a p-value of 0.05. In contrast, there was no adhesion between the non-mineralized material with HAp binding peptides and the cartilage sample in tensile testing giving it a modulus of less than 0.01 MPa. Overall, the bonded samples with mineralization were modestly weaker in tension but demonstrated good bonding strength. The samples without mineralization and specimens without collagen binding peptides bonded to cartilage (data not shown) developed minimal tensile strength in tension testing.

4. Discussion

Paramount in understanding the pathomechanisms leading to PTOA is to decipher how localized AMD temporally and spatially propagates into widespread PTOA. Intact cartilage harbors a structural/metabolic reciprocal relationship between the interstitium of the cartilage and the embedded chondrocytes. The cartilage interstitium converts a variety of external loads into physiologically healthy strains that are transmitted to the chondrocytes [19]. In turn, the chondrocytes transduce the favorable physiologic strains and produce appropriate matrix molecules to support the cartilage interstitium. AMD disrupts this reciprocal relationship. Local damage disrupts the cartilage structure, chondrocytes are injured rendering many cells physiologically incompetent, and many chondrocytes die [10,

15, 20, 21]. Structural damage to the cartilage leads to a mechanically incompetent tissue that can no longer transmit healthy strains to the chondrocytes. Abnormal tissue strains are exacerbated by injury-related cartilage swelling and decreased osmolarity in regions of AMD [20, 22].

The material synthesized in this investigation is a novel development for treatment of AMD sustained by cartilage. To the best of our knowledge, this is the first material specifically developed to treat both the mechanical and biologic pathophysiologic components of AMD. The material has not been developed to serve as a long-term cartilage replacement as many others have tried to develop (reviewed by Hettrich et. al.; there are 637 citations in PubMed returned with the search combination of “cartilage defect” and cartilage regeneration) [30]. Instead, this material is designed to execute its mechanical and biologic function, and subsequently mechanically disintegrate into its small (< 12.6K Daltons) non-toxic constituents.

The physical premise for developing this material is to prevent impact-injured chondrocytes from exposure to abnormal cartilage tissue deformation and swelling after an injury in the acute and subacute time periods. Several investigators have shown that healthy chondrocytes subjected to abnormal strain become metabolically dysfunctional or die [14, 16, 18]. Others have shown that healthy chondrocytes exposed to abnormal tissue swelling in surrounding ground substance are metabolically dysfunctional and at risk for chondrocyte death also [20, 22]. It stands to reason that impact-injured chondrocytes would be affected more than healthy chondrocytes under similar adverse mechanical conditions. Chondrocytes in proximity to AMD after an injury would be subjected to both abnormal tissue strains from local disruption of cartilage matrix and local cartilage swelling. We have hypothesized that restoring normal tissue mechanical behavior in proximity to injured chondrocytes at the time of an injury will increase the number of chondrocytes that survive and resume normal metabolic function after an injury. Cartilage impact studies have shown that chondrocytes die within hours by necrosis followed by a wave of cell death occurring by apoptosis ensuing over the next one to two weeks. The copolymer has been developed to remain securely bonded to injured cartilage for the duration of this subacute time period.

Clinical outcome data clearly demonstrate that there is a need for a change in treatment strategy for intraarticular fractures (Figure 1). AMD sustained by cartilage is an obvious target for intervention. Multiple investigations have demonstrated that chondrocytes in impacted cartilage become metabolically dysfunctional or die [6, 7, 9, 13, 14, 16, 31]. Furthermore, the majority of impact-associated chondrocyte death and dysfunction consistently occurs in the regions sustaining the greatest injury adjacent to fracture lines and cartilage matrix cracks [15, 21, 32].

While chondrocyte death has been shown to concentrate around overt matrix damage initially, it has been shown that both chondrocyte death and metabolic dysfunction propagate spatially and temporally after an injury [7, 9, 13, 18]. Several investigators have demonstrated that apoptotic chondrocyte death occurred for at least seven days post-injury [9, 32]. Investigators have also shown that chondrocyte death and dysfunction expand outwardly from the zone of injury into surrounding cartilage [7, 9, 13]. In summary, impact

related chondrocyte death and dysfunction have been clearly shown to concentrate in regions of AMD, and chondrocyte death and dysfunction are active processes that propagate after injury has occurred. Taken together, a therapeutic target exists to prevent propagation of AMD to PTOA by treating cartilage sustaining AMD.

The copolymer developed in this experiment has favorable physical properties that allow it to treat AMD sustained by cartilage. The copolymer exists as a liquid at room temperature, and will form a hydrogel at body temperature. This will allow for it to be injected into an injured joint as a liquid and infiltrate deep into matrix cracks and fracture edges in regions of AMD. Subsequently, the copolymer will physically transition into a gel while binding to cartilage in matrix cracks and in fracture lines through mineralization, allowing the material to remain securely bonded to injured cartilage surfaces in regions of AMD. Finally, the copolymer will photopolymerize creating a local composite material that helps to restore native material properties to damaged cartilage.

In this paper, we have demonstrated the development of a material that has compressive and shear stiffness comparable to bovine cartilage. The shear and compressive moduli were modestly stiffer than cartilage, but these properties can be modulated by modifying the constituent compositions and inorganic content. The copolymer formed secure bonds with cartilage that was demonstrated by shear testing composite samples of the mineralized copolymer bonded to bovine cartilage (Figures 5 and 6). These findings were confirmed by performing direct tensile testing of the mineralized samples bonded to bovine cartilage (Figure 7). The tensile modulus measured 1.0 MPa in bovine cartilage compared to 0.5 MPa in the bovine cartilage bonded to the mineralized material with hydroxyapatite binding peptides or carboxyl end groups (Figure 7). In contrast, there was no adhesion between the non-mineralized material with HAp binding peptides and the cartilage sample in tensile testing. This shows that in situ mineralization is essential for the implant to form a good interface with cartilage. Secure bonding between the copolymer and surrounding cartilage will likely be important in clinical applications which will allow the copolymer to resist pathologic tensile and shear strains in regions of AMD, and also allow the copolymer to resist pathologic localized strains resulting from injury-related swelling of the cartilage.

While the copolymer has been developed to act as a mechanical stabilizing material, it will also serve as a carrier of chondrocyte-enhancing bioagents. Multiple investigations have demonstrated that multiple bioactive agents prevent chondrocyte death and improve chondrocyte biosynthetic function after an injury [9, 13, 32, 33]. In the future, the copolymer can be loaded with a variety of agents that can be delivered directly into the most injured and damaged regions.

5. Conclusions

A novel nanocomposite photopolymerized hydrogel has been developed that will be capable of infiltrating damaged cartilage and potentially restoring native mechanical properties to local damaged tissue after an injury, based on *in vitro* tensile, compressive and shear moduli measurements. In situ mineralization with calcium phosphate nanocrystals significantly enhances the mechanical strength of hydrogels. The nanocrystals reinforce the structure of

the gels, allowing them to withstand greater forces and deformation. Furthermore, the mineralized copolymer securely adheres to the surrounding cartilage that will allow it to restore tensile and shear resistance to load in damaged regions. It is hypothesized that mechanical restoration of damaged cartilage can potentially prevent propagation of chondrocyte dysfunction and death after an injury, that will prevent PTOA.

Acknowledgments

We would like to acknowledge Colin Paul who assisted with a lot of the initial work on this project through the NSF-REU grant EEC 0851519. We would like to acknowledge financial support from the DOE-SULI program that supported Trishelle Copeland-Johnson. Support from the U. Iowa Vice Provost's office and the NIH CORT grant on Post-Traumatic Osteo-Arthritis is gratefully acknowledged.

Literature Cited

1. Honkonen SE. Degenerative arthritis after tibial plateau fractures. J Orthop Trauma. 1995; 9(4):273–7. [PubMed: 7562147]
2. Marsh JL, Weigel DP, Dirschl DR. Tibial plafond fractures. How do these ankles function over time? J Bone Joint Surg Am. 2003; 85-A(2):287–95. [PubMed: 12571307]
3. Matta JM. Fractures of the acetabulum: accuracy of reduction and clinical results in patients managed operatively within three weeks after the injury. J Bone Joint Surg Am. 1996; 78(11):1632–45. [PubMed: 8934477]
4. Ovadia DN, Beals RK. Fractures of the tibial plafond. J Bone Joint Surg Am. 1986; 68(4):543–51. [PubMed: 3957978]
5. Volpin G, Dowd GS, Stein H, Bentley G. Degenerative arthritis after intra-articular fractures of the knee. Long-term results. J Bone Joint Surg Br. 1990; 72(4):634–8. [PubMed: 2380219]
6. Borrelli J Jr, Silva MJ, Zaegel MA, Franz C, Sandell LJ. Single high-energy impact load causes posttraumatic OA in young rabbits via a decrease in cellular metabolism. J Orthop Res. 2009; 27(3): 347–52. [PubMed: 18924142]
7. Clements KM, Burton-Wurster N, Lust G. The spread of cell death from impact damaged cartilage: lack of evidence for the role of nitric oxide and caspases. Osteoarthritis Cartilage. 2004; 12(7):577–85. [PubMed: 15219573]
8. Duda GN, Eilers M, Loh L, Hoffman JE, Kaab M, Schaser K. Chondrocyte death precedes structural damage in blunt impact trauma. Clin Orthop Relat Res. 2001; 393:302–9. [PubMed: 11764363]
9. Hurtig M, Chubinskaya S, Dickey J, Rueger D. BMP-7 protects against progression of cartilage degeneration after impact injury. J Orthop Res. 2009; 27(5):602–11. [PubMed: 18985691]
10. Krueger JA, Thisse P, Ewers BJ, Dvoracek-Driksna D, Orth MW, Haut RC. The extent and distribution of cell death and matrix damage in impacted chondral explants varies with the presence of underlying bone. J Biomech Eng. 2003; 125(1):114–9. [PubMed: 12661204]
11. Mankin HJ. The reaction of articular cartilage to injury and osteoarthritis. N Engl J Med. 1974; 291(24):1285–92. [PubMed: 4610388]
12. Pascual Garrido C, Hakimiyan AA, Rappoport L, Oegema TR, Wimmer MA, Chubinskaya S. Anti-apoptotic treatments prevent cartilage degradation after acute trauma to human ankle cartilage. Osteoarthritis Cartilage. 2009; 17(9):1244–51. [PubMed: 19332178]
13. Baars DC, Rundell SA, Haut RC. Treatment with the non-ionic surfactant poloxamer P188 reduces DNA fragmentation in cells from bovine chondral explants exposed to injurious unconfined compression. Biomech Model Mechanobiol. 2006; 5(2–3):133–9. [PubMed: 16520961]
14. Chen CT, Burton-Wurster N, Borden C, Hueffer K, Bloom SE, Lust G. Chondrocyte necrosis and apoptosis in impact damaged articular cartilage. J Orthop Res. 2001; 19(4):703–11. [PubMed: 11518282]
15. Lewis JL, Deloria LB, Oyen-Tiesma M, Thompson RC Jr, Ericson M, Oegema TR Jr. Cell death after cartilage impact occurs around matrix cracks. J Orthop Res. 2003; 21(5):881–7. [PubMed: 12919877]

16. Chen CT, Burton-Wurster N, Lust G, Bank RA, Tekkopele JM. Compositional and metabolic changes in damaged cartilage are peak-stress, stress rate and loading-duration dependent. J Orthop Res. 1999; 17(6):870–9. [PubMed: 10632454]
17. Jeffrey JE, Aspden RM. The biophysical effects of a single impact load on human and bovine articular cartilage. Proc Inst Mech Eng (H). 2006; 220 (6):677–86. [PubMed: 16961187]
18. Morel V, Quinn TM. Short-term changes in cell and matrix damage following mechanical injury of articular cartilage explants and modelling of microphysical mediators. Biorheology. 2004; 41(3–4):509–19. [PubMed: 15299282]
19. Guilak F, Jones WR, Ting-Beall HP, Lee GM. The deformation behavior and mechanical properties of chondrocytes in articular cartilage. Osteoarthritis Cartilage. 1999; 7(1):59–70. [PubMed: 10367015]
20. Bush PG, Hodkinson PD, Hamilton GL, Hall AC. Viability and volume of in situ bovine articular chondrocytes-changes following a single impact and effects of medium osmolarity. Osteoarthritis Cartilage. 2005; 13(1):54–65. [PubMed: 15639638]
21. Milentijevic D, Helfet DL, Torzilli PA. Influence of stress magnitude on water loss and chondrocyte viability in impacted articular cartilage. J Biomech Eng. 2003; 125(5):594–601. [PubMed: 14618918]
22. Narmoneva DA, Wang JY, Setton LA. Nonuniform swelling-induced residual strains in articular cartilage. J Biomech. 1999; 32(4):401–8. [PubMed: 10213030]
23. Barei DP, Nork SE, Mills WJ, Coles CP, Henley MB, Benirschke SK. Functional outcomes of severe bicondylar tibial plateau fractures treated with dual incisions and medial and lateral plates. J Bone Joint Surg Am. 2006; 88(8):1713–21. [PubMed: 16882892]
24. Olson SA, Bay BK, Chapman MW, Sharkey NA. Biomechanical consequences of fracture and repair of the posterior wall of the acetabulum. J Bone Joint Surg Am. 1995; 77(8):1184–92. [PubMed: 7642663]
25. Enlow D, Rawal A, Kanapathipillai M, Schmidt-Rohr K, Mallapragada S, Lo CT, et al. Synthesis and characterization of self-assembled block copolymer templated calcium phosphate nanocomposite gels. Journal of Materials Chemistry. 2007; 17:1570–8.
26. Kanapathipillai M, Yusufoglu Y, Rawal A, Hu YY, Lo CT, Thiyaigarajan P, et al. Synthesis and characterization of ionic block copolymer templated calcium phosphate nanocomposites. Chemistry of Materials. 2008; 20:5922–32.
27. Yusufoglu Y, Hu Y, Kanapathipillai M, Kramer M, Kalay YE, Thiyagarajan P, et al. Bioinspired synthesis of self-assembled calcium phosphate nanocomposites using block copolymer-peptide conjugates. Journal of Materials Research. 2008; 23:3196–212.
28. Bali D, King L, Kim S. Synthesis of new gramicidin A derivatives. Aust J Chem. 2003; 56:293.
29. Zeng F, Lee H, Allen C. Epidermal growth factor conjugated poly(ethylene glycol)-block-poly(d-valerolactone) copolymer micelles for targeted delivery of chemotherapeutics. Bioconj Chem. 2006; 17:399.
30. Hettrich CM, Crawford D, Rodeo SA. Cartilage repair: third-generation cell-based technologies--basic science, surgical techniques, clinical outcomes. Sporta Med Arthrosc. 2008; 16(4):230–5.
31. Green DM, Noble PC, Ahuero JS, Birdsall HH. Cellular events leading to chondrocyte death after cartilage impact injury. Arthritis Rheum. 2006; 54(5):1509–17. [PubMed: 16649187]
32. D'Lima DD, Hashimoto S, Chen PC, Colwell CW Jr, Lotz MK. Human chondrocyte apoptosis in response to mechanical injury. Osteoarthritis Cartilage. 2001; 9(8):712–9. [PubMed: 11795990]
33. Martin JA, McCabe D, Walter M, Buckwalter JA, McKinley TO. N-Acetylcysteine Inhibits Post-Impact Chondrocyte Death in Osteochondral Explants. J Bone Joint Surg Am. 2009 In press.

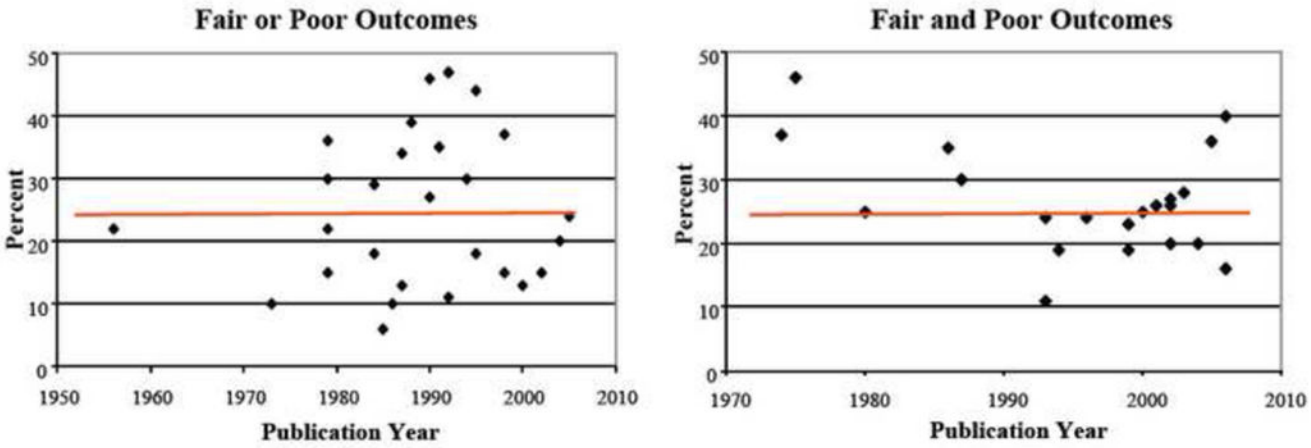

Figure 1.

Fair and poor outcomes for tibial plateau fractures (left) and acetabular fractures (right). Results have seen no improvement for decades.

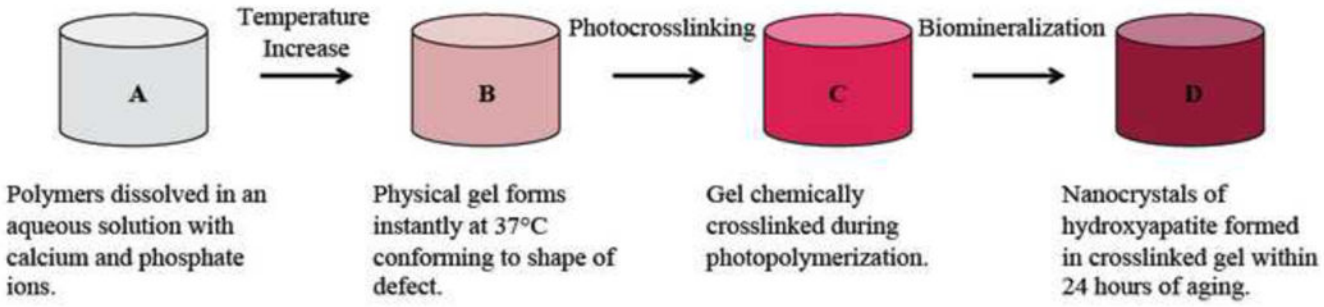

Figure 2.

Schematic depicting the synthesis procedure for the fully mineralized hydrogel. It progresses to cartilage-like material properties once it is fully mineralized.

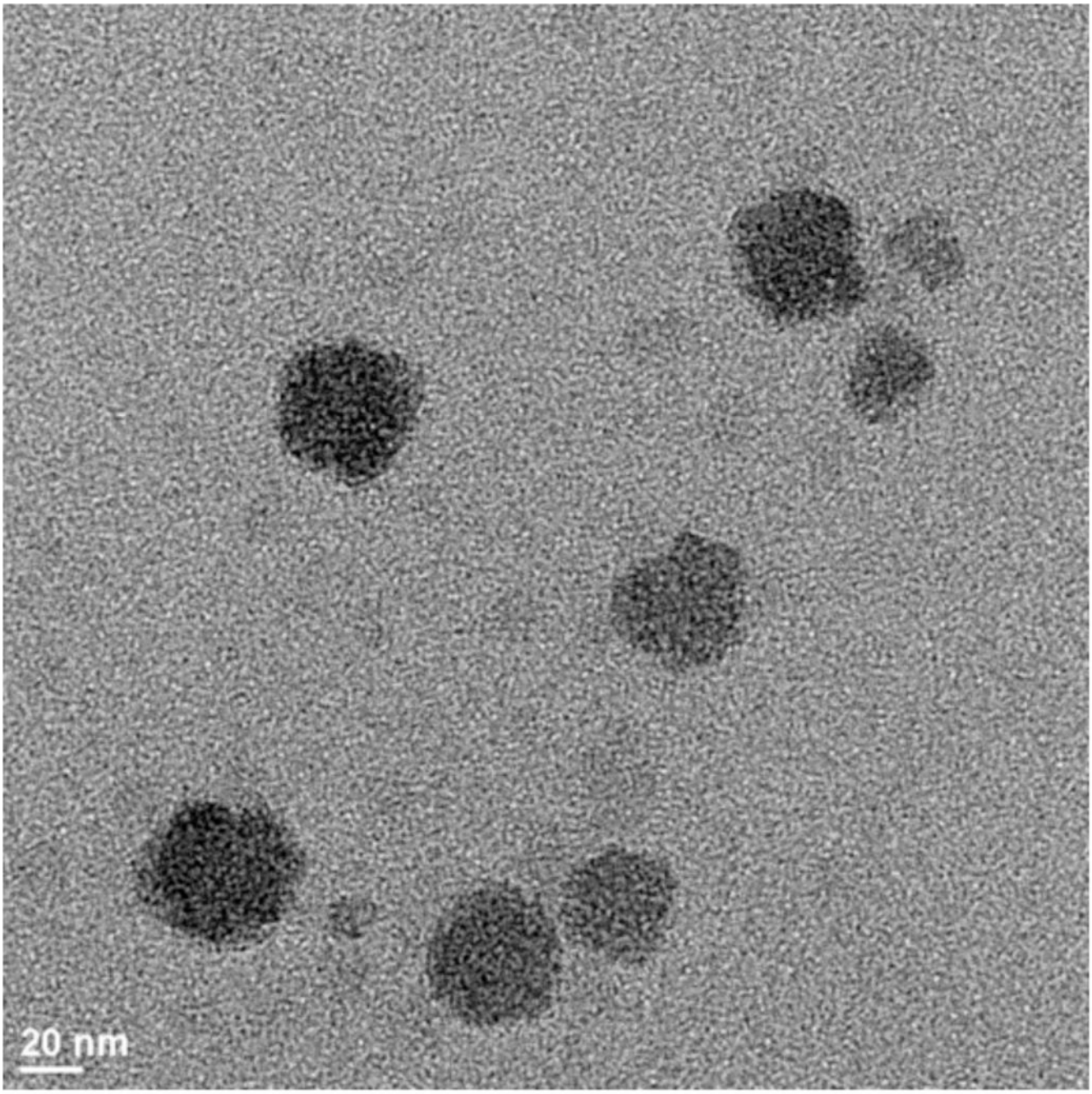

Figure 3.
Bright field Transmission Electron Micrograph obtained at the magnification of 64,000. The average particle size is approximately 40 nm.

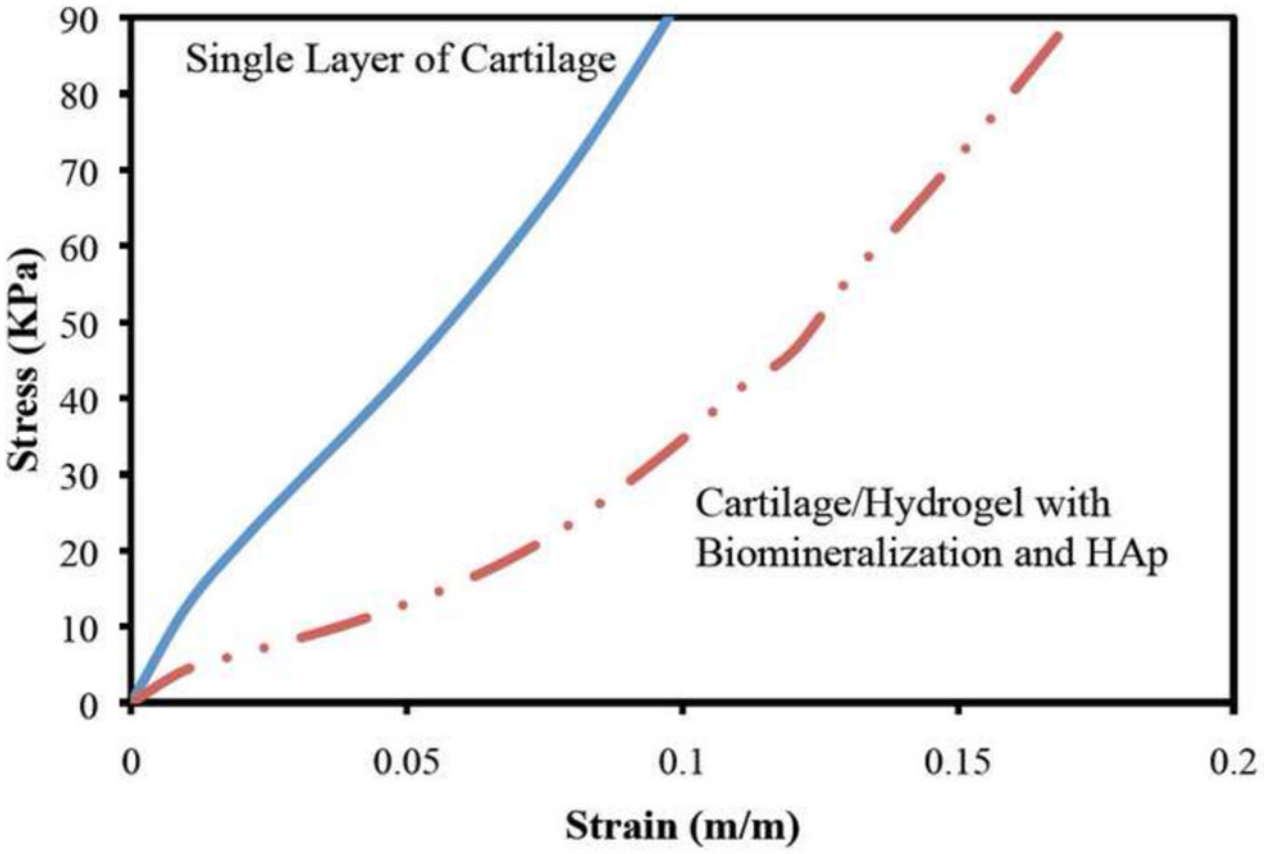

Figure 4.

Compressive stress-strain load deformation on an average of five samples for articular bovine cartilage and cartilage/hydrogel interface specimens. The single layer of articular cartilage (blue) performed similarly to the hydrogel with HAp ( ) and cartilage/hydrogel system with HAp ( ). No significant difference was seen with addition of CBP with ( ) and without ( ) the cartilage interface.

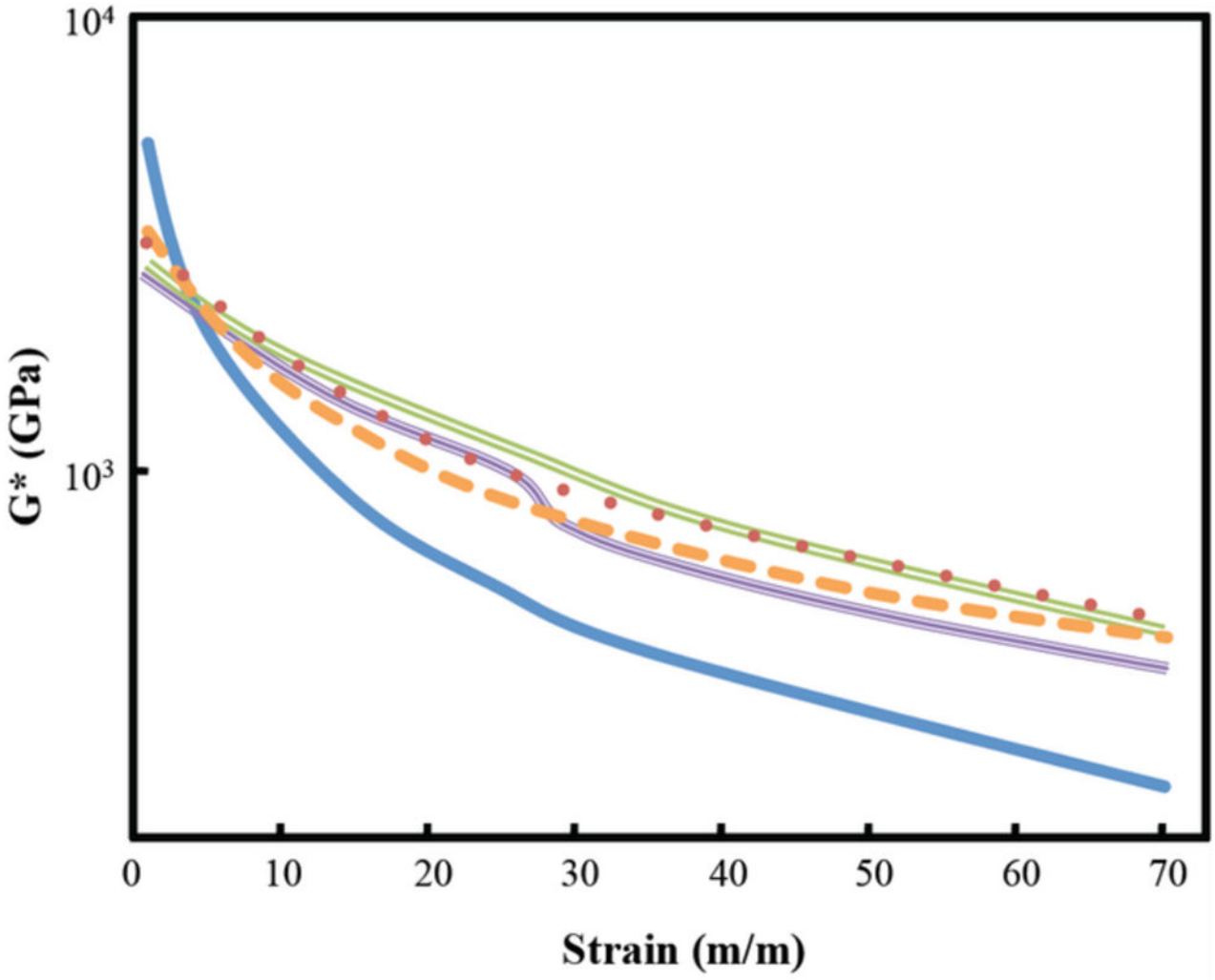

Figure 5.

Shear modulus of four mineralized samples and control bovine cartilage. The experimental samples are stiffer in shear strength from the cartilage ( ). The HAp/CBP samples with ( ) and without ( ) the cartilage interface are slightly stiffer than just the HAp counterpart with ( ) and without ( ) the cartilage interface.

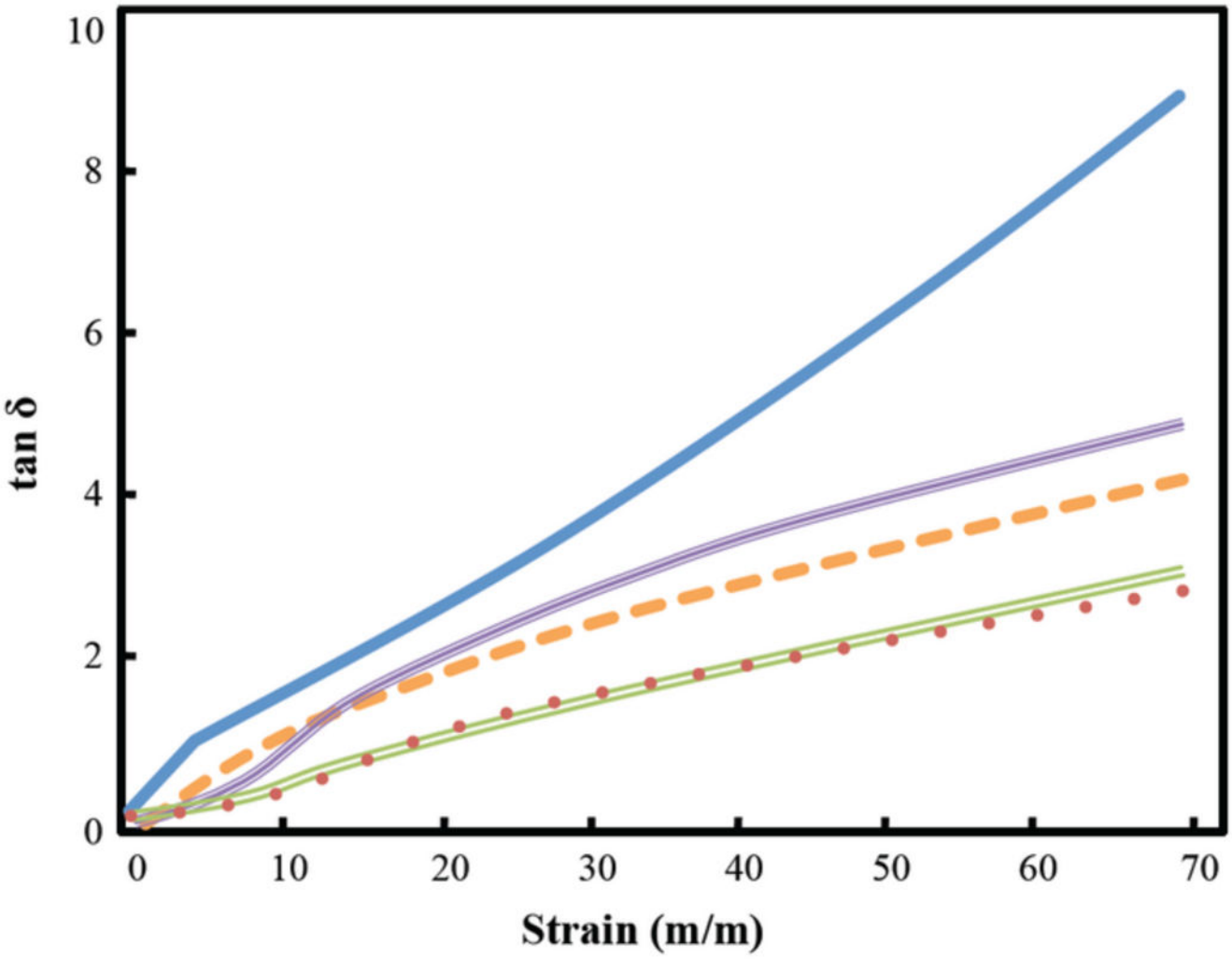

Figure 6.

Tan δ response of four mineralized experimental samples and bovine cartilage. The experimental samples have less of phase angle than the cartilage ( ). The samples with HAp ( ) and CBP ( ) without the cartilage interface have a larger loss to storage ratio than the corresponding HAp ( ) and CBP ( ) samples with the interface.

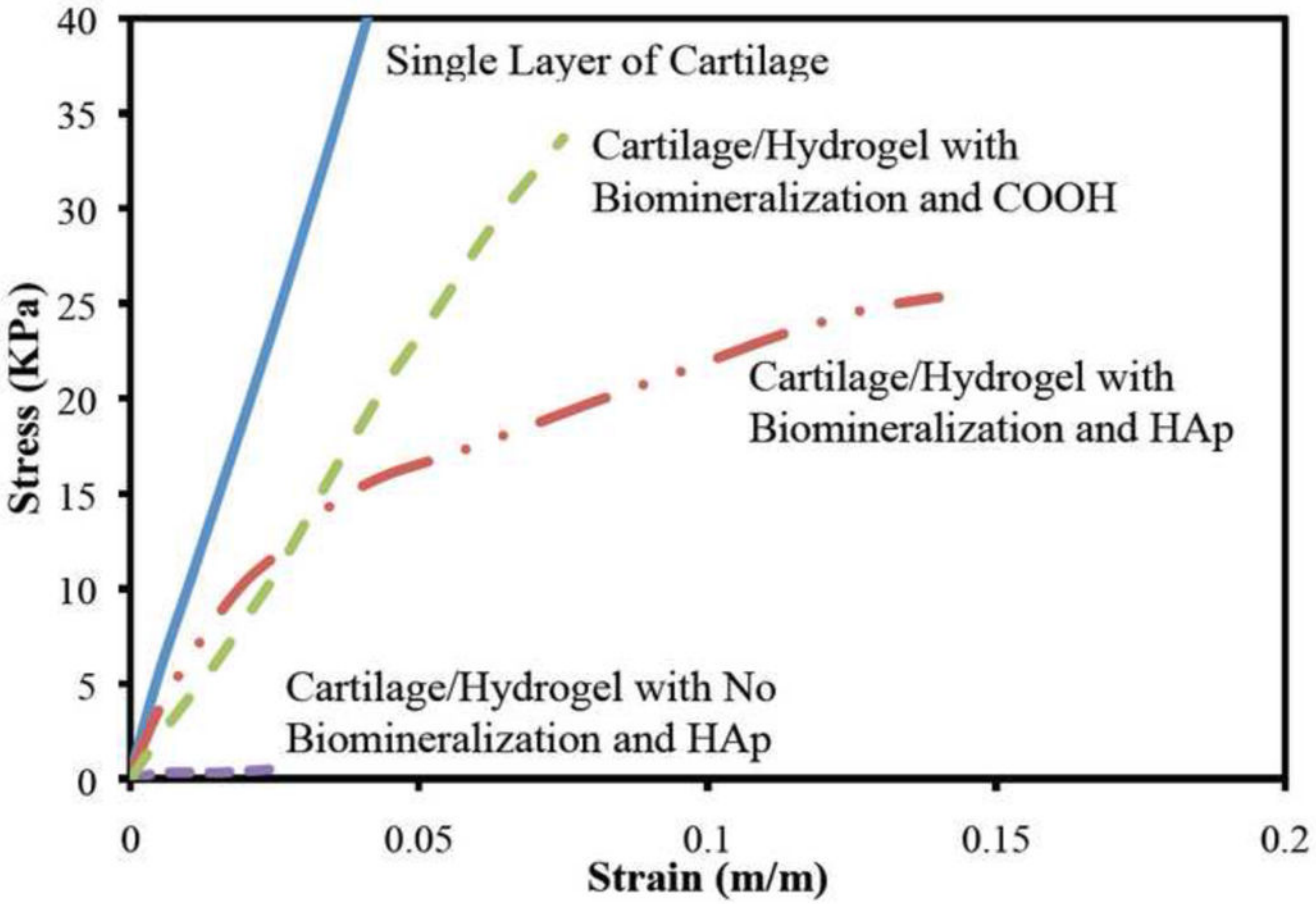

Figure 7.

Average tensile strength of four samples of the mineralized hydrogel with HAp bonded to cartilage, mineralized hydrogel with carboxyl end groups bonded to cartilage, and not mineralized hydrogel with HAp bonded to cartilage compared to tensile strength of bovine cartilage.